XLI CILAMCE
XLI Ibero-Latin American Congress on Computational Methods in Engineering
16-19 November, 2020 FOZ DO IGUAÇU PARANÁ - BRAZIL

Numerical study of CHS-SHS and CHS-RHS T-joints with chord web failure

Daniel J. R. Pereira[1], João B. S. Neto[1], Luiza G. V. Alves[1], Messias J. L. Guerra[2], Gabriel V. Nunes[3], Arlene M. C. Sarmanho[1]

[1]*Dept. of Civil Engineering, Federal University of Ouro Preto (UFOP), Morro do Cruzeiro Campus, 35400-000, Ouro Preto - MG, Brazil*
drocha044@gmail.com, joaobatista011@gmail.com, lluizavasconcellos@gmail.com, arlene@ufop.edu.br
[2]*Dept. of Civil Engineering, Federal Institute of Minas Gerais (IFMG) – Santa Luiza Campus*
junioguerra@hotmail.com
[3]*Dept. of Civil Engineering, Federal Institute of Minas Gerais (IFMG) – Congonhas Campus*
gabriel.nunes@ifmg.edu.br

Abstract. Hollow steel sections have properties that enable their use in large span structures and trusses, in which the design of joints between chords and braces with hollow steel sections are composed of circular (CHS), rectangular (RHS) or square (SHS) cross-sections. However, the current design prescriptions do not contemplate the design of T-joints with containing slender cross-sections. In this work, CHS-SHS and CHS-RHS T-joints with brace-to-chord ratios equal to one and composed of chords with slender sections were analysed through a numerical analysis using a commercial software. A brace axial load of compression was applied, and the normal tension distributions, the joint resistance and the load-displacement behaviour were examined. The numerical results were compared with a design equation from a normative prescription. Chord web failure was observed in all the joints analysed. Thus, the joints outside the current validity ranges of the normative prescriptions – that is, with slender sections – presented the same predicted failure mode for joints with compact or semi-compact cross-sections. The comparison between numerical and analytical joint resistances showed that current design equation does not adequately predict the joint behaviour of joints with slender chords.

Keywords: Hollow steel sections, Joints, Chord web failure, Slender sections.

1 Introduction

The use of truss structures with hollow steel sections (HSS) can be an appropriate choice for several conditions, specially structures with wide spans, since HSS can offer high resistance to axial and loads torsional loads [1].

In the development of the design equations for HSS joints, the validity ranges of these equations were established in tests using mainly circular hollow sections (CHS) and rectangular hollow sections (RHS), with fewer articles involving neither square hollow sections (SHS) nor the combination of CHS-SHS joints.

Furthermore, joints containing chords with high slenderness values were excluded from the design in normative prescriptions and design guides. Thus, more recent researches have studied joints with slender sections; Pereira *et al.* [2] and Guerra *et al.* [3] observed that T-joints with brace-to-chord ratios lower than 0.85 and outside the current validity ranges of the principal design codes presented the same failure mode – chord face plastification – as joints inside these validity ranges.

The same observation was made by Neto *et al.* [4] regarding T-joints with brace-to-chord ratios equal to one, that presented web chord failure. Furthermore, in the study of K-joints, Fleischer *et al.* [5] observed the possibly of broadening the European validity ranges for joints with hollow sections, while Lima *et al.* [6] and Gomes *et al.* [7] have studied reinforcements for T-joints with brace compressive loading.

In this context, this work aimed to determine the failure mode and joint resistance of brace loaded CHS-SHS and CHS-RHS T-joints with brace-to-chord ratios equal to one and containing chords with high slenderness,

though a numerical finite elements (FE) analysis in a commercial software. Furthermore, compare the numerical results with the analytical equation available in NBR 16239 [8].

2 Joint properties

The geometric properties of the joints were defined according to the nomenclature exhibited in Figure 1, where the parameters β and 2γ indicated the brace-to-chord ratio and the cross-section slenderness, respectively. In this work, in all cases, the cross-section height was higher or equal to the chord width; therefore, 2γ indicated the ratio of h_0/t_0.

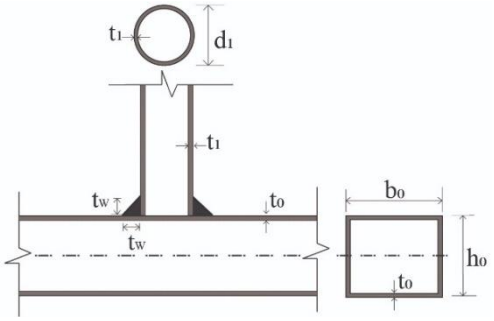

b_0 – width of the chord
h_0 – height of the chord
t_0 – wall thickness of the chord
d_1 – diameter of the brace
t_1 – wall thickness of the brace
$\beta = d_1/b_0$ – brace-to-chord ratio
$2\gamma = b_0/t_0$, $2\gamma = h_0/t_0$ - slenderness ratio

Figure 1. Geometry of a CHS-RHS T-joint

The geometric properties of the joints in this study were shown in Table 1. Fourteen models with 1.0m long chords and 0.3m long braces were analyzed, with variations of the chord height (h_0) and the chord thickness (t_0), what caused the variation of the non-dimensional parameter 2γ. This variation enabled the analysis of the effect of the chord slenderness in the joint resistance in two different series: Series 1 containing CHS-SHS joints and Series 2 containing CHS-RHS joints. The brace thickness varied according to the chord thickness to avoid any failure mode in the brace and did not affect the parameter β nor the parameter 2γ in the joint analysis.

Table 1. Geometric properties of the joints

Series	Model	Geometric properties					Parameters	
		b_0 (mm)	h_0 (mm)	t_0 (mm)	d_1 (mm)	t_1 (mm)	β (d_1/b_0)	2γ (h_0/t_0)
1	1	120	120	3.0	120	3.0	1.0*	40.0*
	2			3.5		3.5		34.3*
	3			4.0		4.0		30.0
	4			4.5		4.5		26.7
	5			5.0		5.0		24.0
	6			5.5		5.5		21.8
	7			6.0		6.0		20.0
2	8		140	3.0		3.0		46.7*
	9			3.5		3.5		40.0*
	10			4.0		4.0		35.0*
	11			4.5		4.5		31.1
	12			5.0		5.0		28.0
	13			5.5		5.5		25.5
	14			6.0		6.0		23.3

*Outside de validity ranges of NBR 16239 [8].

The design of these joints is currently present in several design guides, such as ISO 14346 [9] and NBR 16239 [8]; the latter was the one used in the comparisons in this work, with the validity ranges shown in Table 2.

The nominal material properties used in this study were shown in Table 3. A bilinear diagram with a tangent modulus (E_t) of E/100 – that is, considering strain hardening – was used for braces and chords, while a tangent modulus was not considered for the welds.

Table 2. Validity ranges of NBR 16239 [8]

Condition	Axial loading	Limit
Brace-to-chord ratio	-	$0.4 \le d_1/b_0 \le 0.8$
CHS brace	Compression	$d_1/t_1 \le 0.05\,E/f_y$
RHS chord	Tension	$h_0/t_0 \le 35$
	Compression	$h_0/t_0 \le \begin{cases} 36 \\ 1.45\sqrt{E/f_y} \end{cases}$

Table 3. Material properties

Poisson's ratio ν	Young's modulus (GPa)			Yield strength (MPa)		
	E	Tangent E_t	Weld E_w	Chord f_{y0}	Brace f_{y1}	Weld f_w
0.3	200	E/100	405	300	300	450

3 Numerical model

A computational model using FE analysis in a commercial software was developed. This model was created using Ansys [10], that enabled the development of models using the Ansys Parametric Design Language.

The three elements – brace, chord and weld – of the joint were modelled with the geometric and material properties described. The modeling was made considering solid elements, that enable the simulation of plastic behavior in HSS joints [11]. The weld leg size was considered 1.5 times the chord thickness, what is the minimum recommended by NBR 16239 [8].

The element SOLID185 was used, which contains three degrees of freedom per node and eight nodes, and was an element previously adopted in other researches involving HSS joints [2], [12], [13]; SOLID185 contains plasticity, hyperelasticity, stress stiffening, creep, large deflection, and large strain capabilities [10].

The meshed FE model was more refined in the joint region – medium mesh size of 2mm –, where failure was expected from brace loading. Two fixed ends were the boundary conditions simulated, with translations and rotations restricted through nodes, that were coupled to properly distribute the conditions in all nodes at the ends. The static analysis consisted of brace compressive loading with displacement increments, using the Newton-Raphson iterative method.

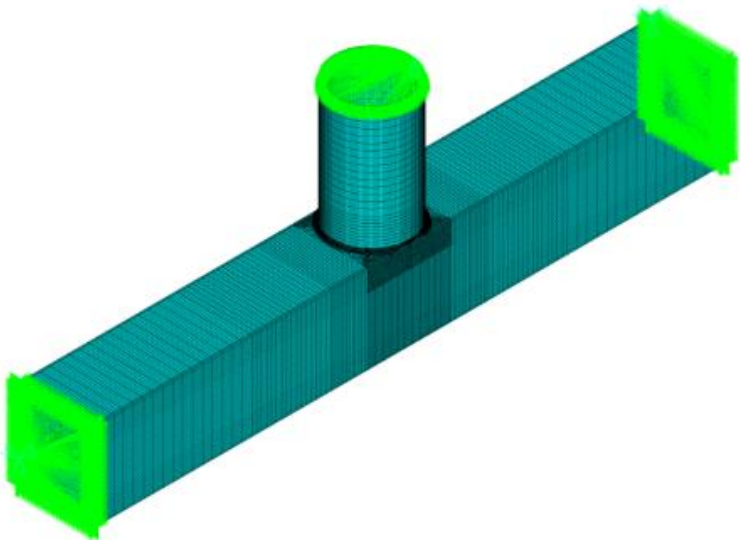

Figure 2. Meshed FE model with node coupling at the ends

4 Results

4.1 Deformation limit criterion

The deformation limit criterion is a method to determine numerical joint resistance loads in HSS [14], [15]. For the joints analyzed in this work, the maximum displacements in the joint (Δ) – Figure 3 – were compared with the peak load: if the peak load occured before a 3%h_0 deformation, the peak load was taken as the joint resistance,; otherwise, the load at a 3%h_0 deformation was considered as the joint resistance.

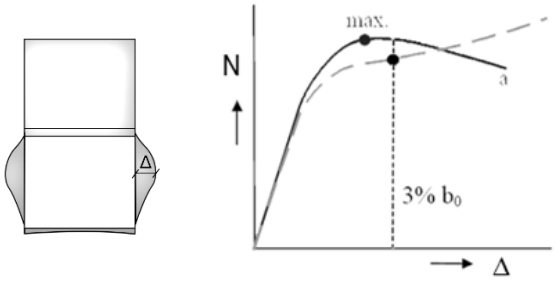

Figure 3. Deformation limit [16]

4.2 Failure mode and von Mises stress distribution

Chord web failure was observed in the joints, since the maximum displacements occured in the lateral faces of the chords and the braces did not present lateral displacments, as it is observable in Figure 4, that showed the von Mises normal stresses distribution in the models.

Bending moments caused normal stresses in the joint region as well as lower chord face displacements, as observable in Figure 4 (b). The normal stresses were higher in the joint region, especially in the encounter of welds and chords.

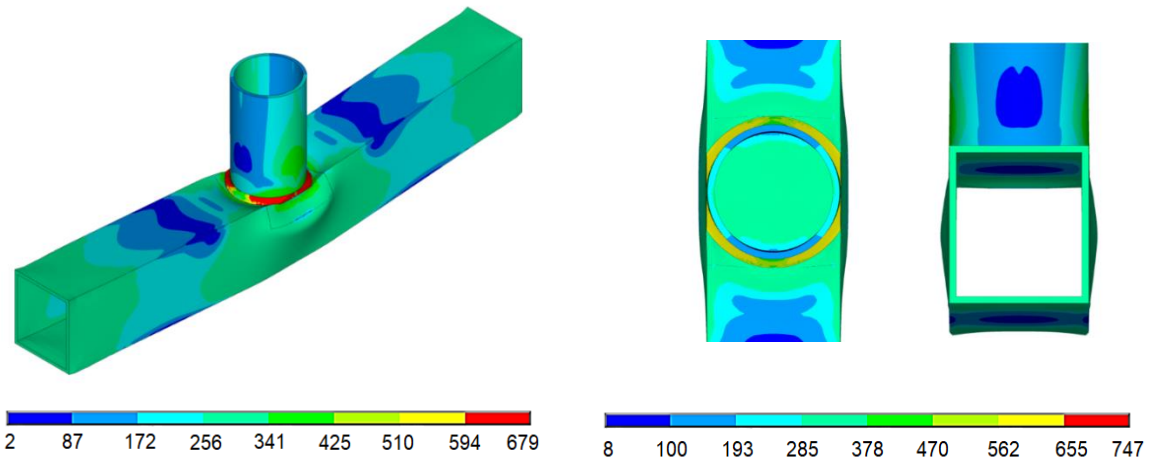

(a) Final displacements applied (b) 3%h_0 stage in Model 14

Figure 4. von Mises tension distribution in perspective (MPa)

The load-displacement curves were shown in Figure 5 for both series, considering the points where the maximum lateral displacements occured. Models 5, 6 and 7 presented a peak load and the analysis was stopped by the software, with the post-yielding behavior not presented. Since the peak load was achieved and used in this work to determine the joint resistance, these values were considered in the comparison.

The peak loads were clearly higher in models with lower 2γ values. When comparing the two series, models in Series 2 presented higher peak loads, what could be explained by higher values of inertia due to higher chord heights.

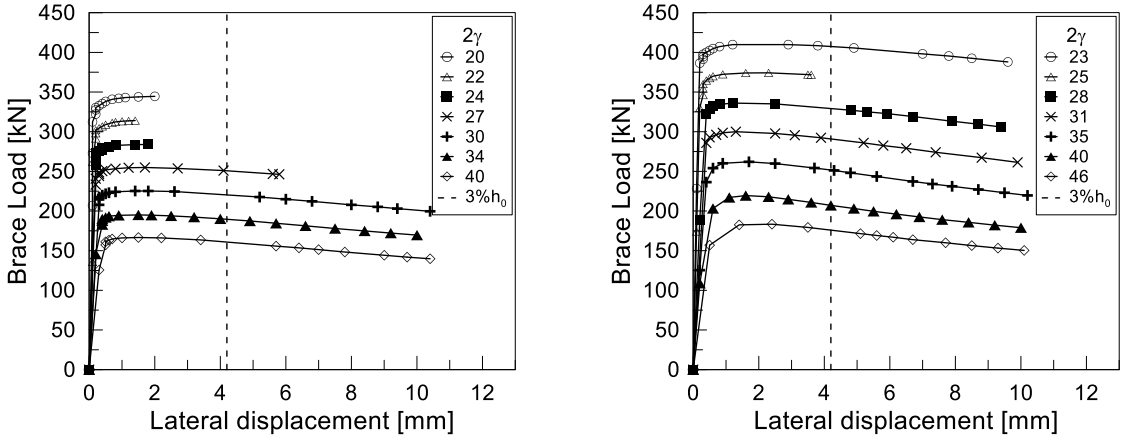

(a) Series 1 (b) Series 2

Figure 5. Load-displacement results.

5 Comparison of results

According to NBR 16239 [8], the design equation – eq. (1) – that determines the joint resistance ($N_{1,Rd}$) for CHS-RHS and CHS-SHS T-joints depends on the stress strength of the chord steel (f_b), that is determined through the multiplication of the yield strength (f_y) by the reduction factor for relevant buckling mode (χ) – eq. (2).

$$\boldsymbol{N}_{1,Rd} = \frac{1}{\gamma_{a1}} f_b t_0 \;\; 2.2 d_1 + 11 t_0 \;\; \frac{\pi}{4} \tag{1}$$

$$f_b = \chi f_y \tag{2}$$

In Table 4, the numerical and analytical ($N_{1,Rk}$) results from eq. (1) were presented, desconsidering the poderation factor γ_{a1} in the calculus.

Table 4. Results and comparison

Model			N_{num} (kN)	Comparison		
Series	Model	2γ		χ	$N_{1,Rk}$ (kN)	$N_{1,Rk}/N_{num}$
1	1	40.0*	166.6	0.33	70.1	0.42
	2	34.3*	195.0	0.45	112.8	0.58
	3	30.0	225.2	0.55	159.8	0.71
	4	26.7	254.8	0.63	209.1	0.82
	5	24.0	283.9	0.69	259.9	0.92
	6	21.8	314.1	0.74	311.9	0.99
	7	20.0	344.6	0.78	364.5	1.06
2	8	46.7*	183.4	0.24	50.7	0.28
	9	40.0*	219.5	0.33	83.3	0.38
	10	35.0*	262.0	0.44	126.7	0.48
	11	31.1	300.0	0.52	174.3	0.58
	12	28.0	336.0	0.60	224.6	0.67
	13	25.5	374.2	0.66	276.6	0.74
	14	23.3	409.9	0.71	329.9	0.80

*Outside de validity ranges of NBR 16239 [8].

The higher discrepancies from analytical and numerical results were observed in models with higher

slenderness (2γ) values. From the results, it was noted that the discrepancies had a trend of diminishing as the 2γ values also decreased.

The numerical joint resistance values were always higher than the analytical results, except for Model 7. Models in Series 2 presented higher joint results than models in Series 1.

6 Conclusions

Chord web failure was the predominant failure mode in all joints, which presented peak loads in the load-displacement curves with maximum deformations occurring in the lateral chord face.

This showed that the joints outside the current validity ranges of the normative prescriptions – that is, with slender sections – presented the same predicted failure mode for joints with compact or semi-compact cross-sections.

The comparison between numerical and analytical joint resistances showed that current joint resistance equation from NBR 16239 [8] does not adequately predict the joint behaviour of CHS-RHS and CHS-SHS T-joints with slender chords and brace-to-chord ratios equal to one.

CHS-RHS joints presented higher joint results than CHS-SHS joints, mostly likely due to higher moment of inertia resistances.

Further experimental and numerical studies with brace loading and chord loading would be necessary to adequately determine an equation for joint resistance of the joints analysed.

Acknowledgements. This work was made with the support from Coordenação de Aperfeiçoamento de Pessoal de Nível Superior – Brasil (CAPES) – Finance code 001, Universidade Federal de Ouro Preto (UFOP), Instituto Federal de Minas Gerais (IFMG), and Conselho Nacional de Desenvolvimento Científico e Tecnológico (CNPq).

Authorship statement. The authors hereby confirm that they are the sole liable persons responsible for the authorship of this work, and that all material that has been herein included as part of the present paper is either the property (and authorship) of the authors, or has the permission of the owners to be included here.

References

[1] A. H. M. de Araújo, A. M. C. Sarmanho, E. de M. Batista, J. A. V. Requena, R. H. Fakury, e R. J. Pimenta, *Projeto de estruturas de edificações com perfis tubulares de aço*, 1º ed. Belo Horizonte: Editora Vallourec, 2016.

[2] D. J. R. Pereira, A. M. C. Sarmanho, G. V. Nunes, M. J. L. Guerra, e V. N. Alves, "Effect of fillet welds on T-joints with thin-walled chords", *Proc. Inst. Civ. Eng. - Struct. Build.*, vol. 172, nº 4, p. 301–312, abr. 2019.

[3] M. J. L. Guerra, A. M. C. Sarmanho, G. V. Nunes, D. J. R. Pereira, e J. B. da S. Neto, "Numerical analysis of 'T' joints with thin walled hollow sections", *Rev. Estrut. do Aço*, vol. 6, nº 2, p. 124, 2017.

[4] J. B. da S. Neto, D. J. R. Pereira, A. M. C. Sarmanho, M. J. L. Guerra, e L. G. V. Alves, "Ligações tubulares sujeitas à plastificação da face lateral do banzo", in *VI CONENGE*, 2019, p. 1663–1677.

[5] O. Fleischer, R. Puthli, T. Ummenhofer, e J. Wardenier, "Axially loaded K joints made of thin-walled rectangular hollow sections", in *Tubular Structures XV*, Batista, Vellasco, e Lima, Orgs. Rio de Janeiro: CRC Press, 2015, p. 457–464.

[6] L. R. O. Lima, L. C. B. Guerrieiro, P. C. G. da S. Vellasco, L. F. Costa-Neves, A. T. da Silva, e M. C. Rodrigues, "Experimental and numerical assessment of flange plate reinforcements on square hollow section T joints", *Thin-Walled Struct.*, vol. 131, p. 595–605, out. 2018.

[7] N. V. Gomes, L. R. O. de Lima, P. C. G. da S. Vellasco, A. T. da Silva, M. C. Rodrigues, e L. F. Costa-Neves, "Experimental and numerical investigation of SHS truss T-joints reinforced with sidewall plates", *Thin-Walled Struct.*, vol. 145, p. 106404, dez. 2019.

[8] NBR 16239, *Projeto de estruturas de aço e de estruturas mistas de aço e concreto de edificações com perfis tubulares*. Rio de Janeiro: Associação Brasileira de Normas Técnicas, 2013.

[9] ISO 14346, *Static design procedure for welded hollow-section joints - Recommendations*. Genebra: International Organization for Standardization, 2013.

[10] ANSYS Inc., *ANSYS 12.1*. EUA: Swanson Analysis System, 2011.

[11] G. J. Van Der Vegte, J. Wardenier, e R. S. Puthli, "FE analysis for welded hollow-section joints and bolted joints", *Proc. Inst. Civ. Eng. - Struct. Build.*, vol. 163, nº 6, p. 427–437, 2010.

[12] L. Lima *et al.*, "Recent advances in tubular joints experiments in Brazil", *Stahlbau*, vol. 87, nº 4, p. 355–362, abr. 2018.

[13] X.-D. Bu e J. A. Packer, "Chord end distance effect on RHS connections", *J. Constr. Steel Res.*, vol. 168, p. 105992, maio 2020.

[14] L. H. Lu *et al.*, "Ultimate deformation criteria for uniplanar connections between I-beam and RHS columns under in-plane bending", *Proc. Fourth Int. Offshore Polar Eng. Conf.*, vol. 4, p. 73–80, 1994.

[15] X.-L. Zhao, "Deformation limit and ultimate strength of welded T-joints in cold-formed RHS sections", *J. Constr. Steel Res.*, vol. 53, nº 2, p. 149–165, 2000.
[16] J. Wardenier, J. A. Packer, X.-L. Zhao, e G. J. van der Vegte, *Hollow sections in structural applications*. Geneva: CIDECT, 2010.